NEOPLASIA
www.neoplasia.com

Volume 11 Number 11 November 2009 pp. 1165–1173 1165

Chaperone-Targeting Cytotoxin and Endoplasmic Reticulum Stress–Inducing Drug Synergize to Kill Cancer Cells[1,2]

Joseph M. Backer*, Arcadius V. Krivoshein*, Carl V. Hamby†, John Pizzonia‡, Kenneth S. Gilbert*, Yonaton S. Ray*, Harrison Brand*, Adrienne W. Paton§, James C. Paton§ and Marina V. Backer*

*SibTech, Inc, Brookfield, CT 06804, USA; †New York Medical College, Valhalla, NY 10595, USA; ‡FujiFilm Medical Systems USA, Inc, Woodbridge, CT 06525, USA; §School of Molecular and Biomedical Science, University of Adelaide, Adelaide, SA 5005, Australia

Abstract

Diverse physiological and therapeutic insults that increase the amount of unfolded or misfolded proteins in the endoplasmic reticulum (ER) induce the unfolded protein response, an evolutionarily conserved protective mechanism that manages ER stress. Glucose-regulated protein 78/immunoglobulin heavy-chain binding protein (GRP78/BiP) is an ER-resident protein that plays a central role in the ER stress response and is the only known substrate of the proteolytic A subunit (SubA) of a novel bacterial AB_5 toxin. Here, we report that an engineered fusion protein, epidermal growth factor (EGF)–SubA, combining EGF and SubA, is highly toxic to growing and confluent epidermal growth factor receptor–expressing cancer cells, and its cytotoxicity is mediated by a remarkably rapid cleavage of GRP78/BiP. Systemic delivery of EGF-SubA results in a significant inhibition of human breast and prostate tumor xenografts in mouse models. Furthermore, EGF-SubA dramatically increases the sensitivity of cancer cells to the ER stress–inducing drug thapsigargin, and *vice versa*, demonstrating the first example of mechanism-based synergism in the action of a cytotoxin and an ER-targeting drug.

Neoplasia (2009) 11, 1165–1173

Introduction

Mammalian cells use evolutionarily conserved protective mechanisms that attenuate stress induced by physiological and therapeutic insults. Selective inhibition of such stress responses in cancer cells can provide a foundation for effective anticancer therapy. This might be particularly true for the unfolded protein response (UPR) that manages endoplasmic reticulum (ER) stress induced by various drugs, oxygen and glucose deprivation, alterations in Ca^{2+} fluxes, and by inhibition of protein degradation. Initiation of the UPR is controlled by an ER chaperone, glucose-regulated protein 78/immunoglobulin heavy-chain binding protein (GRP78/BiP) [1,2]. Most GRP78/BiP resides inside the ER lumen, although a certain fraction of the protein spans the ER membrane, and in some cells, a fraction of the protein is in the outer cell membrane [1,2]. Under normal conditions, GRP78/BiP molecules are distributed between two main functions: 1) serving as chaperones for newly synthesized proteins that are folded in the ER and 2) sequestering the ER luminal domains of the ER stress transducers activating transcription factor 6, inositol-requiring enzyme 1, and PKR-like ER kinase. Under ER stress conditions that lead to enhanced production of misfolded/unfolded proteins, GRP78/BiP distribution is shifted toward its chaperone functions. As a result, released stress transducers initiate the UPR program, leading to activation of a complex interplay of survival and death signals, one of which

Abbreviations: EGF, epidermal growth factor; EGFR, epidermal growth factor receptor; scVEGF, single-chain vascular endothelial growth factor; ER, endoplasmic reticulum; EGF-SubA, fusion protein combining EGF and SubA; GRP78/BiP, glucose-regulated protein 78/immunoglobulin heavy-chain binding protein; SubA, subtilase-like proteolytic subunit of bacterial AB_5 toxin; UPR, unfolded protein response

Address all correspondence to: Marina V. Backer, SibTech, Inc, 115A Commerce Dr, Brookfield, CT 06804. E-mail: mbacker@sibtech.com

[1]This study was funded by the National Institutes of Health grant 1R43CA132349-01A2 (M.V.B.).

[2]This article refers to supplementary materials, which are designated by Figures W1 to W7 and are available online at www.neoplasia.com.

Received 28 May 2009; Revised 10 July 2009; Accepted 13 July 2009

DOI 10.1593/neo.09878

leads to enhanced GRP78/BiP expression. If up-regulation of GRP78/BiP is sufficient to handle both unfolded proteins and ER stress transducers, the cell survives. Alternatively, if ER stress persists, the cell dies.

Recently, it has been reported that GRP78/BiP is the only known substrate of a novel bacterial AB_5-type cytotoxin SubAB [3,4]. SubAB comprises a single A subunit (SubA) with subtilisin-like proteolytic activity and a pentamer of targeting B subunits. Surprisingly, although partial inhibition of GRP78/BiP expression, through antisense or RNA interference approaches, does not affect cell growth [5–7], SubA-induced cleavage of GRP78/BiP leads to cell death [4]. We reasoned that targeted delivery of SubA through receptor-mediated endocytosis might be a suitable strategy for assaulting tumor cells, which often overexpress GRP78/BiP [1]. It should be noted that nearly all bacterial or plant toxins explored for cancer therapy so far, such as truncated diphtheria toxin (DT) or Shiga-like toxin (StxA), worked through the inhibition of protein synthesis [8]. We hypothesized that because of its unique mechanism of action, SubA might synergize with ER stress–inducing drugs, resulting in a more severe insult to cancer cells.

To test this hypothesis, we fused SubA to epidermal growth factor (EGF), whose receptor (EGFR) is frequently overexpressed in tumor cells, and evaluated the resulting EGF-SubA fusion protein *in vitro* and *in vivo*. We report here that EGF-SubA acts synergistically with drugs that significantly upregulate BiP expression, providing a possibility of the development of combination regimens for effective anticancer therapy.

Materials and Methods

Construction of EGF-SubA Fusion Protein

DNA encoding the enzymatic subunit of SubAB (SubA) without a leader sequence (a M1-A21 N-terminal fragment) was amplified by polymerase chain reaction (PCR) from the pK184/SubA plasmid encoding the full-length subunit A [4] and cloned in-frame with a codon-optimized human EGF cDNA (kindly provided by Dr. P. T. Pienkos, Molecular Logix, Woodlands, TX) into the pET/Hu-R4C$(G_4S)_3$ vector for bacterial expression of proteins with Cys-tag [9,10]. EGF-SubA and three control proteins (SubA, EGF-ciSubA, and EGF-StxA described in Figure W1) were expressed in *Escherichia coli* strain BL21 (DE3), recovered from inclusion bodies and refolded through dialysis under RedOx conditions as described for Cys-tagged proteins [9]. All proteins were purified through ion exchange chromatography (1-ml prepacked Sepharose FF columns; GE Healthcare, Waukesha, WI).

Fluorescent Tracers

SH-directed modification of Cys-tagged proteins was done according to the standard protocol [9]. Briefly, the reactive SH group of C4 in Cys-tag was activated by a 20-minute treatment with equimolar DTT in 0.1 M Tris-HCl pH 8.0 at 25°C and then reacted for 1 hour at 25°C with a maleimide derivative of a fluorescent dye as follows. To develop fluorescent EGF-SubA*, EGF-SubA was reacted with a one molar equivalent of Alexa Fluor 594 maleimide (Invitrogen, San Diego, CA) and purified by gel filtration on Ultrogel AcA 202 (Pall BioSepra, France). To synthesize fluorescent scVEGF*, single-chain vascular endothelial growth factor (scVEGF) [9,10] was reacted with a 1.5-fold molar excess of Alexa Fluor 594 maleimide and purified by reverse-phase high-pressure liquid chromatography on a protein C-4 column (Vydac, Hesperia, CA). Cys-tagged EGF [10] was modified with a twofold molar excess of Oregon Green 488 maleimide (OrG; Invitrogen) and was purified on PD-10 column (GE Healthcare), resulting in a fluorescent EGF-OrG tracer. The protein concentrations of the fluorescent tracers were determined from integral intensity peaks on reverse-phase high-pressure liquid chromatography profiles at 214 nm. The concentrations of Alexa Fluor 594 and Oregon Green 488 were determined spectrophotometrically. The functional activity of all fluorescent tracers was tested in tissue culture as described [10,11] and was found to be no less than 80% of the corresponding unmodified protein.

Tissue Culture

MDA231luc cells were developed and cultured as described [10]. F98-EGFR, F98-EGFR(F), and F98 rat glioma cells (kindly provided by Dr. R. Barth, the Ohio State University) were maintained in 50:50 (vol%) Dulbecco's modified Eagle medium/F-12 (Gibco, Billings, MT) supplemented with 5% FBS (HyClone, Logan, UT) and 2 mM L-glutamine (Gibco). PC3 and MCF-7 cells (obtained from ATCC, Manassas, VA) were maintained in F-12 (Sigma, St. Louis, MO) or minimum essential medium (Gibco), respectively, with 10% FBS and 2 mM L-glutamine. U266-B1 cells (obtained from ATCC) were grown in RPMI (Sigma), 20% FBS, and 2 mM L-glutamine. All cells were maintained at 5% CO_2 at 37°C.

Cell Growth Inhibition

Cells were plated in 96-well plates at a density of 2000 to 5000 cells per well in 50 μl per well of the corresponding media. Various concentrations of proteins, drugs, or mixtures thereof were added to cells in triplicate wells 20 hours later to make a total volume of 0.1 ml per well, and cells were incubated under standard culture conditions for 72 to 96 hours. Viable F98, F98-EGFR, and F98-EGFR(F) cells and confluent MDA231luc cells were determined using a 3-[4,5-dimethylthiazol-2-yl]-2,5-diphenyltetrazolinium bromide assay (Sigma) according to the manufacturer's instructions. Viable PC3, MCF-7, U266-B1, and subconfluent MDA231luc cells were detected by CellTiter 96 AQueous One Solution Cell Proliferation assay (Promega, Madison, WI). The half-maximal inhibitory concentration (IC_{50}) values were determined by plotting the viable cell numbers (as percent of control) *versus* the concentration of a cytotoxic compound.

Fluorescent Microscopy

F98 and F98-EGFR(F) cells were plated on glass slides in complete culture medium 20 hours before the experiment. Fluorescent EGF-SubA* and control tracers EGF-OrG and scVEGF* were added to cells in complete culture medium to final concentrations of 2 nM and incubated at 37°C for 10 minutes. Cells were washed with PBS, fixed in fresh 4% formaldehyde (Polysciences, Warrington, PA) for 10 minutes at room temperature, and mounted in mounting medium for fluorescence supplemented with 4′,6-diamidino-2-phenylindole (DAPI) for nuclear counterstaining (Vector Laboratories, Burlingame, CA). Slides were observed with a 43× oil objective on a Zeiss Axiovert microscope (Zeiss, Oberkochen, Germany).

Western Blot Analysis

Total protein in clarified cell lysates was determined by a micro-BCA assay (Pierce, Rockford, IL). Equal amounts of total protein (25-40 μg per lane, depending on the antibody) were separated by SDS-PAGE and transferred to nitrocellulose. GRP78/BiP antibody H-129 (sc-13968; Santa Cruz Biotechnology, Santa Cruz, CA) that reacts with the intact BiP and its 28-kDa fragment was used at the

beginning of this work. In the course of the study, the H-129 antibody lost reactivity. After having tested several lots of H-129 from Santa Cruz Biotechnology, none of which showed satisfactory reactivity and specificity, we switched to a different supplier. The rest of the study was done with GRP78/BiP antibody from R&D Systems (Minneapolis, MN; clone 474421, no. MAB4846) that recognizes the intact BiP and its 44-kDa fragment. N-terminal β-actin and phosphotyrosine pY (clone PT-66) antibodies were from Sigma. Ms-Spectrin (nonerythroid, α-fodrin) antibody was from Chemicon (Millipore, Billerica, MA). Cleaved caspase-7 (Asp 198) antibody was from Cell Signaling (Beverly, MA). Active caspase-3 antibody was from AbCam (Cambridge, MA). Secondary HRP-conjugated antibodies and the ECL Plus detection kit were from GE Healthcare. Blot images were captured by a gel documentation system (Streamcare, Rochester, NY) and analyzed by Kodak 1D Image Analysis Software (Kodak, Rochester, NY). Intact BiP signal intensities were normalized to the corresponding β-actin signals.

In-cell Western

Cells were plated onto 96-well Optilux Black/clear bottom tissue culture–treated plates (BD Falcon, Franklin Lakes, NJ) at a density of 20,000 cells per well. EGF-SubA was serially diluted in complete culture medium and added to cells in triplicate wells 20 hours later. Cells were incubated at 37°C for 24 hours then washed once with PBS, fixed in fresh 4% formaldehyde (Polysciences) for 10 minutes at room temperature, permeabilized in PBS/0.1% Triton X-100, and blocked in Odyssey Blocking Buffer (Li-COR, Lincoln, NE) for 2 hours. Active caspase-3 antibody (AbCam) diluted 1:500 was added to cells for 2 hours at room temperature, followed by secondary goat anti–rabbit IRDye-800CW antibody (Li-COR) diluted 1:500 and supplemented with Sapphire700 and DraQ5 (both from Li-COR) for nonspecific cell staining. After 1 hour of incubation, cells were extensively washed with PBS–0.1% Tween-20, air-dried, and scanned simultaneously at 700 and 800 nm using a Starion FLA-9000 imager (FujiFilm Medical Systems, New York, NY). The fluorescent signal of active caspase-3 from each well was quantified and normalized by the total protein content per well.

Fluorescent Apoptosis Assays

Fluorescent apoptosis assays were done as described [12].

Induction of EGFR Tyrosine Phosphorylation

Induction of EGFR tyrosine phosphorylation was done as described [11]. Briefly, F98-EGFR(F) cells were grown in 24-well plates to approximately 80% confluence. After overnight serum starvation, cells were incubated with indicated amounts of EGF (Sigma) or EGF-SubA for 10 minutes, lysed, and analyzed by Western blot analysis with phosphotyrosine-specific antibody (clone PT-66; Sigma).

Mice

Five- to six-week-old severe combined immunodeficient (SCID)/Ncr (BALB/c background) mice were from Charles River Laboratories (Wilmington, MA). Orthotopic breast tumors were established by inoculation of 5×10^6 MDA231luc cells in the region of mouse fat pad. PC3 cells were injected subcutaneously in left flanks at 3×10^6 cells per mouse. Tumors were measured with calipers, and the tumor volume was calculated as $V = 0.52 \times L \times W \times H$. The protocol for the animal studies was reviewed and approved by the Institutional Animal Care and Use Committee at the University of Connecticut Health Center.

Immunohistochemistry

Immunohistochemistry was done as described [10].

Results

EGF-SubA Fusion Protein Cleaves Intracellular GRP78/BiP

EGF-SubA was expressed in *E. coli* as an insoluble protein, refolded, and purified through ion exchange chromatography to more than 95% purity (Figure W2*A*). Rat glioma F98 cells engineered to express 1.4×10^6 human EGFR per cell (F98-EGFR(F) cells; Table 1) were used to test its functional activity. EGF-SubA induced EGFR tyrosine autophosphorylation in F98-EGFR(F) cells, although less efficiently, but still in the same concentration range as recombinant EGF (Figure 1*A*), attesting to the functional activity of the EGF moiety. EGF-SubA retained the proteolytic activity and specificity of the parental bacterial toxin $SubAB_5$, as judged by its ability to cleave recombinant 78-kDa GRP78/BiP between L416 and L417, yielding a 44- and a 28-kDa fragments (Figure 1*B*).

To evaluate EGFR-mediated internalization of EGF-SubA in F98-EGFR(F) cells by fluorescent microscopy, we made a fluorescent tracer EGF-SubA*. EGF-SubA, as well as all control proteins developed for this study (Figure W1), was expressed with a cysteine-containing Cys-tag designed for site-specific conjugation of various payloads [9]. As we previously reported, SH-directed modification of recombinant Cys-tagged growth factors carried out under defined conditions preserves the functional activity of the modified proteins, including their ability to bind to cognate receptors [9–12]. Indeed, we found that site-specifically modified and unmodified EGF-SubA displayed a very similar activity in a standard cytotoxicity assay (Figure W2*B*).

EGF-SubA* accumulated in F98-EGFR(F) cells at low nanomolar concentrations as efficiently as fluorescent EGF (Figure 1*C*). To prove that the observed uptake was EGFR-mediated, and not a result of enhanced endocytic activity of the transfected glioma cells, we used an unrelated growth factor scVEGF* [10] site-specifically labeled with Alexa Fluor 594. scVEGF* administered at the same concentration failed to accumulate in F98-EGFR(F) cells (Figure 1*C*). Another specificity control, F98 cells lacking EGFR expression, did not show any detectable amount of EGF-SubA* even after 1 hour of incubation with as high as 125 nM tracer (Figure 1*C*). These data indicate that bacterially expressed EGF-SubA is capable of rapid and selective accumulation in EGFR-positive cells.

To test EGFR-mediated proteolytic activity of EGF-SubA, we selected human prostate cancer (PC3) and human breast cancer (MDA231luc) cells, both expressing moderate levels of EGFR (approximately 2×10^5 EGFR per cell; Table 1) and similar levels of BiP (Figure W3). EGF-SubA induced rapid cleavage of BiP in these

Table 1. EGF-SubA Toxicity for Cancer Cell Lines with Varying EGFR Expression.

Cell Line	EGF-SubA Toxicity (IC_{50})	EGFR/Cell	Reference
F98 rat glioma	6 nM	None	[36]
F98-EGFR rat glioma	20 pM	10^5	[36]
F98-EGFR(F) rat glioma	20 pM	1.4×10^6	[11]
MCF-7 human breast cancer	5 nM	1.5×10^4	[37]
MDA231luc human breast cancer	30 pM	2×10^5	Figure W2 [38], for MDA-MB-231
PC3 human prostate	1 pM	~2×10^5	Figure W2
U266-B1 human myeloma	>6 nM	None	Figure W2

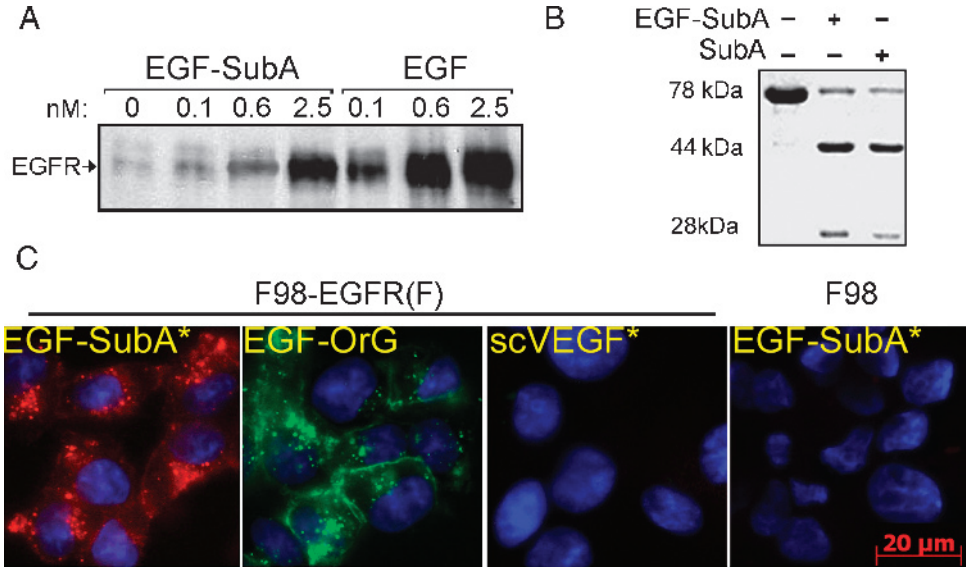

Figure 1. EGF-SubA is functionally active. (A) Induction of EGFR tyrosine phosphorylation in F98-EGFR(F) cells. (B) Cleavage of recombinant BiP followed by reducing SDS-PAGE was done as described [3]. Proteins from the gel were transferred onto polyvinylidene fluoride membrane; the 28-kDa fragments were excised, washed, and subjected to N-terminal sequencing using Edman chemistry on an Applied Biosystems Procise automated sequencer (Foster City, CA). In both cases, the sequence was L-D-V-C-P, which is consistent with cleavage of BiP between L_{416} and L_{417}. (C) Each fluorescent tracer was added to F98-EGFR(F) cells to a final concentration of 2 nM for 10 minutes. EGF-SubA* was added to control F98 cells at a concentration of 125 nM for 1 hour. Red indicates EGF-SubA*; green, EGF-OrG; red, scVEGF*; blue, nuclei (DAPI). Scale bar, 20 μm.

cells (Figure 2, *A* and *B*). However, the time course of EGF-SubA–induced alterations in BiP levels revealed a cell-specific pattern of destruction and *de novo* synthesis of BiP. In PC3 cells, the cleavage was remarkably fast, with a substantial decrease of intact BiP after as short as 5 minutes of the treatment. Band intensity analysis revealed that the amount of intact BiP dropped 14-fold during the first 3 hours of exposure. Notably, the level of intact BiP was not restored in PC3 cells during the 24-hour course of treatment (Figure 2*A*). In contrast, we did not observe any substantial BiP cleavage in MDA231luc until 1.5 hours of exposure (Figure 2*B*). The maximal cleavage in both cell types was reached at the same time (by 3 hours); however, MDA231luc cells, unlike PC3, responded to continuous BiP cleavage by a significant up-regulation of BiP expression. The level of intact BiP in MDA231luc was restored by 9 hours, and by 24 hours of treatment, it was increased approximately twofold over the level of control untreated cells. The inability of an equivalent amount of untargeted SubA to induce BiP cleavage in MDA231luc until 24 hours of treatment (Figure W4*A*) confirmed that EGFR-mediated endocytosis was critical for efficient delivery of EGF-SubA into the cell.

The different susceptibilities of MDA231luc and PC3 cells to EGF-SubA were confirmed by dose-finding experiments, when cells were exposed to varying amounts of EGF-SubA for 72 hours. We found that BiP cleavage and the appearance of a 44-kDa BiP fragment in PC3 cells was detectable at 0.1 pM EGF-SubA, whereas at least a fourfold higher concentration was required for MDA231luc cells (Figure W4*B*).

EGF-SubA Is a Powerful Cytotoxin

The cytotoxicity of SubAB holotoxin was attributed to its ability to selectively cleave BiP [3,4]. In agreement with these data, PC3 cells that displayed the fastest EGF-SubA–induced BiP cleavage seemed to be the most sensitive to EGF-SubA toxicity among all tested cell lines, with an IC_{50} value of 1 pM (Table 1). As expected from Western blot analysis, MDA231luc cells were less sensitive (IC_{50} = 30 pM). To confirm a causative role of BiP cleavage in these effects, we constructed a control fusion protein, EGF-ciSubA, containing a catalytically inactive (ci) mutant of SubA, which failed to inhibit the growth of PC3 cells (Figure W4*C*).

The high cytotoxicity of EGF-SubA for tumor cells was EGFR-dependent because EGFR-negative F98 or U266-B1 cells were 200- to 6000-fold less sensitive to EGF-SubA than MDA231luc or PC3 cells, respectively (Table 1). An EGFR-mediated mechanism of the effects of EGF-SubA on MDA231luc cells was further confirmed by the absence of toxicity of untargeted SubA (Figure 2*C*). These data are in an agreement with a previously published observation that SubA subunit alone, without the targeting B subunit, was not toxic to susceptible Vero cells [4]. Finally, a competition assay, in which EGF rescued cells from EGF-SubA–induced toxicity in a dose-dependent manner (Figure 2*D*), confirmed an EGFR-mediated mechanism of EGF-SubA–induced toxicity.

Although EGFR is necessary to mediate the toxicity of EGF-SubA, the relationship between the levels of EGFR expression and EGF-SubA–induced toxicity is apparently more complex than a simple direct correlation. We found that two EGFR-expressing F98 cell lines, F98-EGF and F98-EGFR(F), displayed the same susceptibility to EGF-SubA, with IC_{50} values of 20 pM each, despite one order of magnitude difference in the EGFR expression levels. Additional evidence was obtained by analyzing two human breast carcinoma cell lines, namely, MDA231luc and MCF-7, with moderate (~2×10^5 EGFR per cell) and low (~10^4 EGFR per cell) EGFR expressions, respectively. The susceptibility of these cells to EGF-SubA differed more than 150-fold, despite only an approximately 20-fold difference in EGFR expression levels.

Interestingly, at low EGF-SubA concentrations, two sequential half doses of cytotoxin given 24 hours apart were more effective

against MDA231luc cells than an equivalent amount given as a single dose (Figure W5). It is possible that the second half dose of EGF-SubA given in 24 hours was more effective than the full dose in blunting a protective cellular response owing to the kinetics of BiP up-regulation in these cells by 24 hours after the first exposure (Figure 2*B*).

Importantly, a 96-hour exposure of 100% confluent MDA231luc cells to EGF-SubA resulted in a dose-dependent decrease in the numbers of viable cells, as judged both by a 3-[4,5-dimethylthiazol-2-yl]-2,5-diphenyltetrazolinium bromide dye assay and by directly counting the cells (Figure 2*E*), indicating that cell growth is not required for EGF-SubA action. In contrast, the activity of other cytotoxins is reported to be dependent on cell growth [13,14]. Indeed, a control fusion of EGF with the A subunit of Shiga toxin (EGF-StxA; Figure W1) was not effective against confluent cells (Figure 2*E*). The EGF and StxA domain activity, as well as the cytotoxicity of EGF-StxA fusion protein for growing MDA231luc cells, was confirmed in separate experiments (Figure W6).

EGF-SubA induced massive apoptosis in PC3 cells, as detected by in-cell Western analysis of active caspase-3 (Figure 2*F*). Similarly, the SubAB holotoxin was reported to induce apoptosis in Vero cells [15].

EGF-SubA Inhibits Tumor Growth

To evaluate the activity of EGF-SubA *in vivo*, we used PC3 and MDA231luc tumors grown in SCID mice. EGF-SubA is a large protein of 45 kDa; therefore, first, we established if it was capable of

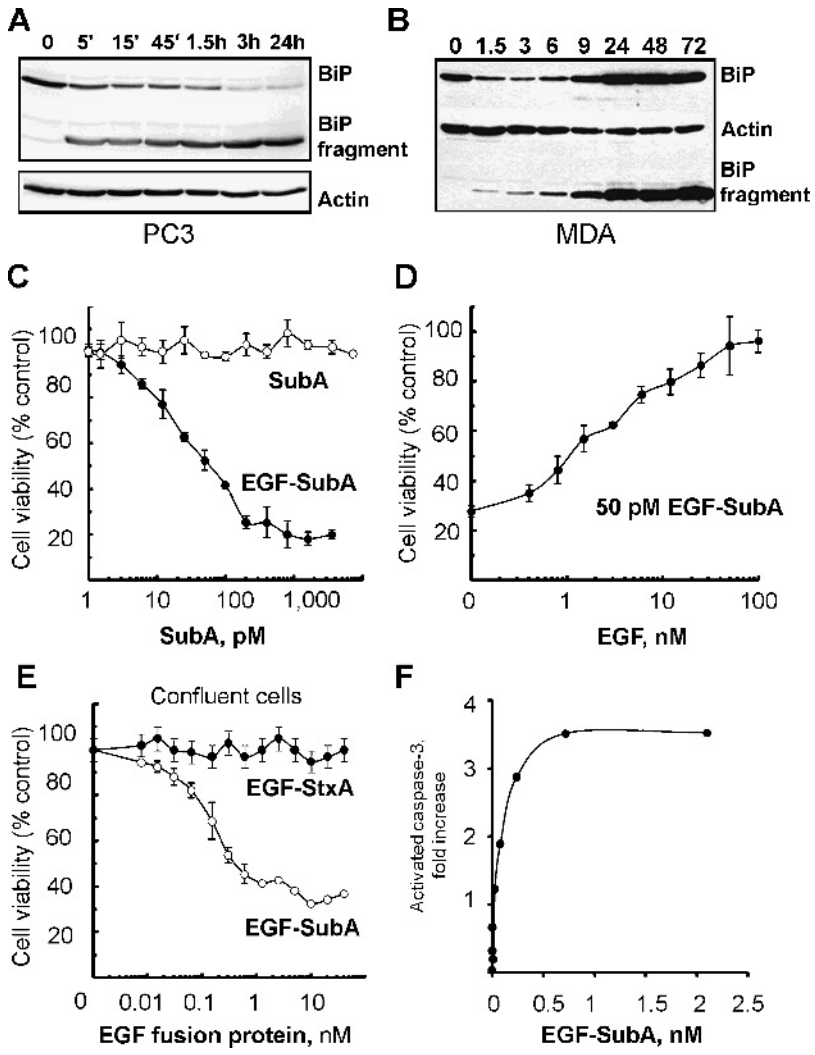

Figure 2. EGF-SubA–induced cytotoxicity is EGFR-dependent. Selective cleavage of BiP in PC3 cells (A) and MDA231luc cells (B). Cells were plated in six-well plates, 0.5 million/well, exposed to 1 nM EGF-SubA 20 hours later. Equal amounts of clarified cytosols (40 μg of total protein) were analyzed by Western blot analysis using antibody specific for BiP from R&D Systems (A) or Santa Cruz Biotechnology (B). (C) MDA231luc cells were plated in triplicate wells of 96-well plates, 2000 cells per well, and exposed to EGF-SubA, or untargeted SubA, 20 hours later. Cell viability was determined after 72 hours. (D) MDA231luc cells were plated as described in panel C. Varying amounts of competitor EGF were mixed with EGF-SubA and added to cells to a final concentration of 50 pM EGF-SubA. Cell viability was determined after 72 hours. (E) Ninety-six hours after plating, after reaching 100% confluence, MDA231luc cells were exposed to EGF-SubA or EGF-StxA. Cell viability was determined after 5 days of treatment. At the highest concentration of EGF-SubA, cells were directly counted in Coulter Counter, and a 66% decrease in the number of treated *versus* control cells (66,800 *vs* 198,000 cells per well) corresponded to the results of the viability assay. (F) In-cell Western analysis of caspase-3 activation in PC3 cells after a 24-hour exposure to varying amounts of EGF-SubA.

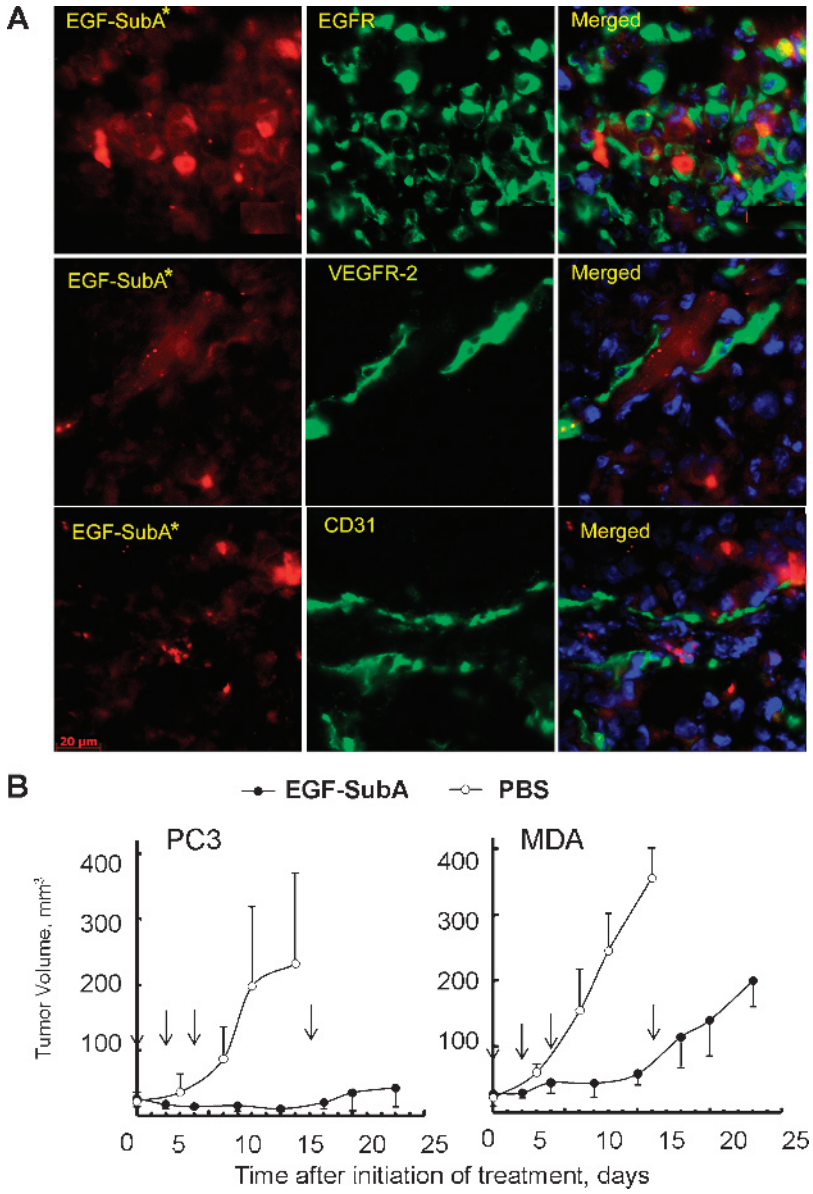

Figure 3. EGF-SubA inhibits tumor growth. (A) MDA231luc tumor-bearing mouse injected intravenously with fluorescent EGF-SubA* (125 μg/kg), 1 hour before termination. To identify cells with red fluorescence, tumor cryosections were stained for EGFR, VEGFR-2, or CD31. Staining was developed with Alexa Fluor 488 by the TSA amplification technique (Molecular Probes, Invitrogen, Carlsbad, CA). Red indicates EGF-SubA*; blue, nuclei (DAPI). (B) Growth of PC3 (left panel) and MDA231luc (right panel) tumors in SCID (Balb/c background) mice. Arrows indicate days of injections with EGF-SubA.

extravasating it from tumor blood vessels and penetrating the tumor tissue. MDA231luc tumor–bearing mice were injected with fluorescent EGF-SubA* (125 µg/kg, intravenously) 1 hour before termination. Fluorescent immunohistochemical analysis of tumor cryosections revealed that most Alexa Fluor 594 fluorescence was associated with EGFR-positive cells within the tumor (EGFR staining; Figure 3*A*), with a small amount associated with endothelial cells in tumor blood vessels (VEGFR-2 and CD31 staining; Figure 3*A*).

To establish if therapeutically relevant amounts of EGF-SubA could be accumulated in tumor tissue, we selected a regimen of several consecutive intraperitoneal (IP) injections, at a dose of 125 µg/kg per injection. After 10 to 12 days of tumor cell implantation, when tumors became palpable, mice (n = 5) received four IP injections of EGF-SubA. The first three injections were done every other day, with the last injection done 1 week after the third injection. Control mice (n = 5) were injected IP with saline. The treatment was well tolerated, with no clinical signs of toxicity observed in any treated groups.

A significant inhibition of tumor growth in both tumor models was detected after the first three injections; however, it did not result in complete tumor regression. Consistent with the results obtained in tissue culture experiments, PC3 tumors seemed to be more responsive to EGF-SubA treatment than MDA231luc tumors (Figure 3*B*). The accumulated experience with EGF-targeted toxins suggests that an increased EGF-SubA dosage could lead to tumor regression but would also result in unacceptable nonspecific organ toxicity. Current approaches to achieving higher cytotoxin efficiency are local delivery and/or PEGylation of the cytotoxin [16]. Another possibility would be combining a cytotoxin with a synergistic drug. We hypothesized

that, owing to its unique mechanism of action, EGF-SubA could synergize with ER stress–inducing drugs.

EGF-SubA Synergizes with a Strong ER Stress Inducer

In searching for a potential synergistic drug, we tested thapsigargin, a known cytotoxic inducer of ER stress [17]. Thapsigargin inhibits ER Ca^{2+}-dependent ATPase, leading to a depletion of ER Ca^{2+} storage, which, in turn, decreases the activity of Ca-dependent chaperones leading to an increase in unfolded proteins and the corresponding induction of UPR signaling. As expected, treatment of MDA231luc with thapsigargin resulted in a time-dependent increase of BiP (Figure 4*A*). However, in cells exposed to a combination of EGF-SubA and thapsigargin, cleavage of BiP led to accumulation of the BiP fragment but not to net up-regulation of the intact protein, as was observed for either thapsigargin (Figure 4*A*) or EGF-SubA alone (Figure 2*B*). Thus, the combination of EGF-SubA and thapsigargin effectively sabotaged the UPR defense mechanism.

To evaluate the relationship between the effects of thapsigargin and EGF-SubA, we used an approach, pioneered by Berenbaum [18], to analyze interactions between the drugs as either additive, synergistic, or antagonistic. In this approach, a mixture of two drugs is prepared at a ratio based on their corresponding IC_{50} values, and then the IC_{50} value for each drug is determined from a dose-dependent experiment with this mixture. If the drugs are additive, it will lead to an approximately twofold decrease in the IC_{50} value for each drug in combination relative to the drugs alone. The sum (S) of fractional IC_{50} (a ratio of IC_{50} for a drug in a combination to IC_{50} for drug alone) serves as a quantitative criterion, indicating synergism when $S < 1$, additivity when $S \sim 1$, and antagonism when $S > 1$. To apply this approach, thapsigargin alone or in combination with EGF-SubA at a molar ratio of 1000:1 was serially diluted in complete culture medium and added to MDA231luc cells. We found that the combination of these two compounds was dramatically more effective than either drug alone ($S = 0.15$), with fractional IC_{50} values of 0.056 for thapsigargin and 0.094 for EGF-SubA, respectively. Synergism between EGF-SubA and thapsigargin was particularly striking because of the essentially nontoxic concentrations of each compound alone, whereas their combination at the same concentrations was extremely cytotoxic (Figure 4*B*).

An analysis of overall caspase activity, as well as the combined activity of executioner caspases-3 and -7, supports a synergistic enhancement of apoptosis by the combination of thapsigargin and EGF-SubA (Figure 4*C*). Further analysis revealed that the EGF-SubA/thapsigargin combination led to an increased cleavage of α-fodrin, a known substrate of caspase-3 [19] but not to a notable increase of the cleaved, activated form of caspase-7 (Figure 4*D*), indicating that the synergistic effect might be preferentially mediated by caspase-3. Interestingly, a 24-hour treatment with EGF-SubA alone did not result in any significant cleavage of α-fodrin or procaspase-7.

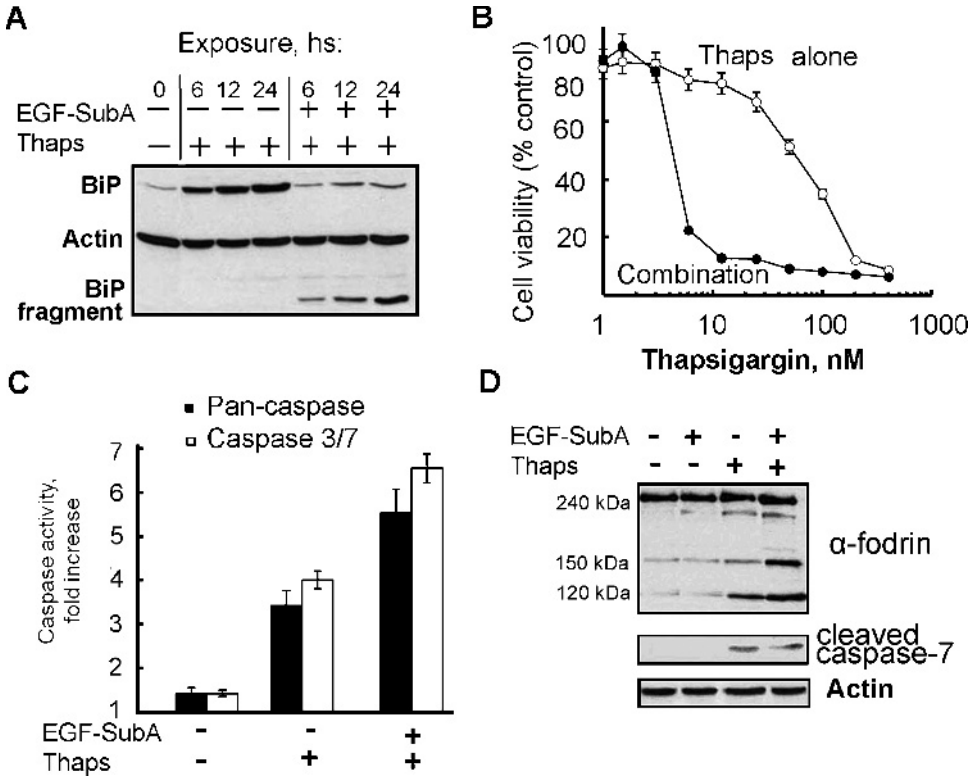

Figure 4. EGF-SubA enhances cytotoxic effects of the ER stress inducer thapsigargin. (A) MDA231luc cells plated in six-well plates, 0.5 million/well, and, 20 hours later, were exposed to 1 nM EGF-SubA, 2.5 μM thapsigargin, or their combination for 18 to 20 hours. Clarified cytosol fractions were analyzed for BiP cleavage as described in the legend to Figure 1 (BiP antibody was from Santa Cruz Biotechnology). (B) MDA231luc cells were plated in 96-well plates at 2000 cells per well. Twenty hours later, cells in triplicate wells were exposed to varying amounts of thapsigargin alone (Thaps) or in combination with EGF-SubA at a molar ratio of 1000:1. Viability was determined 72 hours later. (C and D) MDA231luc cells were plated and treated as in panel A. Clarified cytosols were analyzed for caspase activity using fluorescent pan-caspase AC-2 and specific caspase 3/7 substrates (C) and cleavage of α-fodrin (25 μg total protein per lane) and caspase-7 (40 μg total protein per lane) (D).

To further elucidate the role of BiP up-regulation in response to a EGF-SubA/drug combination, we tested two known chemotherapeutics, doxorubicin and bortezomib. Doxorubicin is not known to induce ER stress, whereas bortezomib inhibits protein degradation by proteosomes and induces ER stress and the UPR in some experimental systems [20]. When tested on MDA231luc cells, neither doxorubicin nor bortezomib was very effective in the induction of BiP up-regulation (Figure W7*A*), particularly when compared with thapsigargin (Figure 4*A*). Using the same approach as described above for the EGF-SubA/thapsigargin combination, we observed marginally synergistic interactions between EGF-SubA and either bortezomib or doxorubicin (Figure W7, *B* and *C*), with the corresponding sums of fractional IC_{50} values S = 0.7 and 0.8. Thus, it seems that a significant up-regulation of BiP is a specific requirement for synergism in EGF-SubA/drug combinations.

Discussion

We report here that EGF-SubA is cytotoxic to both growing and confluent EGFR-expressing cells in the picomolar concentration range and that cytotoxicity is mediated by BiP cleavage. The changes in BiP level in response to an EGF-SubA–induced insult progress through a rapid and significant decline followed by up-regulation of BiP production. In this respect, despite different routes of intracellular delivery, EGF-SubA is similar to the bacterial SubAB holotoxin [3,21]. The magnitude of the response to EGF-SubA varied across the group of EGFR-positive cells evaluated in this study, and EGF-SubA–induced toxicity did not directly correspond to the EGFR expression level. Most likely, this reflects a more complex interplay between such cell-specific processes as EGFR/ligand clathrin- and non–clathrin-mediated internalization and trafficking [22] and the magnitudes of ER stress and UPR signaling in a particular cell line. The results obtained in tissue culture translated well in animal tumor models. The ability of EGF to compete with EGF-SubA for binding to EGFR in tissue culture might indicate a possible limitation of EGF-SubA applicability *in vivo*. However, the accumulated experience with EGF-toxin fusion proteins [8,16], as well as multiple publications on targeted *in vivo* imaging of tumor EGFR with EGF-based tracers [10, and supplementary material herein; 23,24] suggests that EGF-SubA would successfully compete with endogenous EGF for binding to and internalization into EGFR-positive tumor cells *in vivo*.

The dependence on GRP78/BiP for cell survival is cell specific [25,26]. Suzuki et al. [27] demonstrated that two of seven tested cell lines, PC3 and HeLa, underwent apoptosis after transfection with GRP78/BiP siRNA. However, for most cancer cell lines, down-regulation of GRP78/BiP through antisense and RNA interference approaches is not cytotoxic [5–7]. We reason that the rapid cleavage of BiP, as opposed to slower down-regulation through antisense and RNAi methods, is primarily responsible for the irreversible cytotoxic effects of EGF-SubA. Mechanistically, it is possible that the rapid release of ER stress transducers activating transcription factor 6, inositol-requiring enzyme 1, and PKR-like ER kinase, as reported recently for the SubAB holotoxin [15], cannot be efficiently compensated by slower up-regulation of GRP78/BiP expression or by other protective pathways. Alternatively, the cleavage of GRP78/BiP might result in the opening of translocation pores in the ER, for example, at the luminal end of the Sec61 translocon pore [28], which, in turn, activates additional mechanisms of cell destruction.

Our main finding is that treating cells undergoing ER stress with EGF-SubA has a potent synergistic effect on cellular cytotoxicity. In contrast, the combinations of EGF-SubA with drugs that do not induce ER stress produce mostly additive effects. A logical explanation for such selective synergism would be the ability of EGF-SubA to sabotage cell reliance on GRP78/BiP in developing a protective response to ER stress [29]. This is the first example of mechanism-based synergism in the action of immunotoxin and ER-targeting drugs, and it provides a new paradigm for the rational design of combination regimens for anticancer therapy. Importantly, such therapy would target not only EGFR-positive cancer cells but also EGFR-expressing tumor endothelial cells [30].

Is there translational significance in our findings? So far, attempts to use targeted immunotoxins have distinctively mixed records [8,16]. Problems with systemic toxicity, aggravated by preexisting immunity, prevented or terminated clinical development of several immunotoxins, including EGF-DT [31–33]. The preexisting immunity to DT moiety originates from diphtheria-tetanus-pertussis vaccine that provides for a high immunization level and a long-memory immune response. Indeed, 25% of the breast cancer patients involved in EGF-DT phase 1/2 clinical trials had high pretreatment DT antibody titers, and all patients had high DT-specific antibody titers 1 month after treatment [34]. From this standpoint, EGF-SubA is a more suitable candidate for clinical development.

Nevertheless, ER stress inducers, such as thapsigargin or tunicamycin, also display unacceptable systemic toxicity, and their formulation might require reengineering either as targeted drugs or prodrugs [17]. Our results suggest that EGF-SubA in combination with synergistic ER stress–inducing drugs might be effective at significantly lower doses than required for monotherapy. Furthermore, a nonlinear decrease in sensitivity to EGF-SubA cells observed for cells with low physiological levels of EGFR expression may provide an additional level of safety for normal tissue. Because EGFR overexpression is associated with invasiveness and metastatic potential of tumor cells [35], we suggest that EGF-SubA/drug combinations might be particularly effective against metastatic tumors. Given the additional advantages of cytotoxic activity against confluent cells and the absence of preexisting immunity to SubAB, targeting BiP with EGF-SubA or other targeted SubA cytotoxins might provide unique translational opportunities for a rational mechanism-based design of combination treatments.

Acknowledgments

Codon-optimized human EGF was kindly provided by P. T. Pienkos (Molecular Logix, Woodlands, TX). F98, F98-EGFR, and F98-EGFR (F) cells were generously provided by R. Barth (The Ohio State University, Columbus, OH). The authors thank A. S. Lee (University of Southern California Keck School of Medicine, University of Southern California/Norris Comprehensive Cancer Center, Los Angeles, CA) for critical reading of the manuscript.

Competing Interests Statement

J. M. Backer owns equity in privately held SibTech, Inc.

References

[1] Lee AS (2007). GRP78 induction in cancer: therapeutic and prognostic implications. *Cancer Res* **67**, 3496–3499.

[2] Xu C, Bailly-Maitre B, and Reed JC (2005). Endoplasmic reticulum stress: cell life and death decisions. *J Clin Invest* **115**, 2656–2664.

[3] Paton AW, Beddoe T, Thorpe CM, Whisstock JC, Wilce MCJ, Rossjohn J, Talbot UM, and Paton JC (2006). AB5 subtilase cytotoxin inactivates the endoplasmic reticulum chaperone BiP. *Nature* **443**, 548–552.

[4] Paton AW, Srimanote P, Talbot UM, Wang H, and Paton JC (2004). A new family of potent AB(5) cytotoxins produced by Shiga toxigenic *Escherichia coli*. *J Exp Med* **200**, 35–46.

[5] Tsutsumi S, Namba T, Tanaka KI, Arai Y, Ishihara T, Aburaya M, Mima S, Hoshino T, and Mizushima T (2006). Celecoxib upregulates endoplasmic reticulum chaperones that inhibit celecoxib-induced apoptosis in human gastric cells. *Oncogene* **25**, 1018–1029.

[6] Dong D, Ko B, Baumeister P, Swenson S, Costa F, Markland F, Stiles C, Patterson JB, Bates SE, and Lee AS (2005). Vascular targeting and antiangiogenesis agents induce drug resistance effector GRP78 within the tumor microenvironment. *Cancer Res* **65**, 5785–5791.

[7] Zu K, Bihani T, Lin A, Park YM, Mori C, and Ip C (2006). Enhanced selenium effect on growth arrest by BiP/GRP78 knockdown in p53-null human prostate cancer cells. *Oncogene* **25**, 546–554.

[8] Pastan I, Hassan R, Fitzgerald DJ, and Kreitman RJ (2006). Immunotoxin therapy of cancer. *Nat Rev Cancer* **6**, 559–565.

[9] Backer MV, Levashova Z, Levenson R, Blankenberg FG, and Backer JM (2008). Cysteine-containing fusion tag for site-specific conjugation of therapeutic and imaging agents to targeting proteins. *Methods in Molecular Medicine: Peptide-Based Drug Design*. L Otvos (Ed.). New York, NY: Humana Press, Vol. 494, pp. 275–294.

[10] Backer MV, Levashova Z, Patel V, Jehning B, Claffey K, Blankenberg FG, and Backer JM (2007). Molecular imaging of VEGF receptors in angiogenic vasculature with single-chain VEGF driven probes. *Nature Med* **13**, 504–509.

[11] Levashova Z, Backer MV, Horng G, Felsher D, Backer JM, and Blankenberg FG (2009). SPECT and PET imaging of EGF receptor with site-specifically labeled EGF and dimeric EGF. *Bioconjug Chem* **20**, 742–749.

[12] Backer MV, Patel V, Jehning BT, Claffey KP, Karginov VA, and Backer JM (2007). Inhibition of anthrax protective antigen outside and inside the cell. *Antimicrob Agents Chemother* **51**, 245–251.

[13] Backer MV and Backer JM (2001). Targeting endothelial cells overexpressing VEGFR-2: selective toxicity of Shiga-like toxin-VEGF fusion proteins. *Bioconjug Chem* **12**, 1066–1073.

[14] Veenendaal LM, Jin H, Ran S, Cheung L, Navone N, Marks JW, Waterberger J, Thorpe P, and Rosenblum MG (2002). *In vitro* and *in vivo* studies of a VEGF121/rGelonin chimeric fusion toxin targeting the neovasculature of solid tumors. *Proc Natl Acad Sci USA* **99**, 7866–7871.

[15] Wolfson JJ, May KL, Thorpe CM, Jandhyyala DM, Paton JC, and Paton AW (2008). Subtilase cytotoxin activates PERK, IRE and ATF6 endoplasmic reticulum stress–signaling pathways. *Cell Microbiol* **10** (9), 1775–1786.

[16] Kreitman RJ (2006). Immunotoxins for targeted cancer therapy. *AAPS J* **8** (3), E532–E551.

[17] Denmeade SR and Isaacs JT (2005). The SERCA pump as a therapeutic target: making a "smart bomb" for prostate cancer. *Cancer Biol Ther* **4**, 14–22.

[18] Berenbaum MC (1978). A method for testing synergy with any number of agents. *J Infect Dis* **137**, 122–130.

[19] Cohen GM (1997). Caspases: the executioners of apoptosis. *Biochem J* **326**, 1–16.

[20] Nawrocki ST, Jennifer S, Carew JS, Dunner KJ, Boise LH, Chiao PJ, Huang P, Abbruzzese JL, and McConkey DJ (2005). Bortezomib inhibits PKR-like endoplasmic reticulum (ER) kinase and induces apoptosis via ER stress in human pancreatic cancer cells. *Cancer Res* **65**, 11510–11519.

[21] Lass A, Kujawa M, McConnell E, Paton AW, Paton JC, and Wójcik C (2008). Decreased ER-associated degradation of a-TCR induced by Grp78 depletion with the SubAB cytotoxin. *Int J Biochem Cell Biol* **40** (12), 2865–2879.

[22] Le Roy C and Wrana JL (2005). Clathrin- and non–clathrin mediated endocytic regulation of cell signaling. *Nat Rev* **6**, 112–126.

[23] Levashova Z, Backer MV, Horng G, Felsher D, Backer JM, and Blankenberg FG (2009). SPECT and PET imaging of EGF receptor with site-specifically labeled EGF and dimeric EGF. *Bioconjug Chem* **20**, 742–749.

[24] Nitin N, Rosbach KJ, El-Naggar A, Williams M, Gillenwater A, and Richards-Kortum RR (2009). Optical molecular imaging of EGFR expression to improve detection of oral neoplasia. *Neoplasia* **11**, 542–551.

[25] Luo S, Mao C, Lee B, and Lee AS (2006). GRP78/BiP is required for cell proliferation and protecting the inner cell mass from apoptosis during early mouse embryonic development. *Mol Cell Biol* **26**, 5688–5697.

[26] Fu Y, Wey S, Wang M, Ye R, Liao C-P, Roy-Burman P, and Lee AS (2008). Pten null prostate tumorigenesis and AKT activation are blocked by targeted knockout of ER chaperone GRP78/BiP in prostate epithelium. *Proc Natl Acad Sci USA* **105**, 19443–19448.

[27] Suzuki T, Lu J, Zahed M, Kita K, and Suzuki N (2007). Reduction of GRP78 expression with siRNA activates unfolded protein response leading to apoptosis in HeLa cells. *Arch Biochem Biophys* **468**, 1–14.

[28] Alder NN, Shen Y, Brodsky JL, Hendershot LM, and Johnson AE (2005). The molecular mechanisms underlying BiP-mediated gating of the Sec61 translocon of the endoplasmic reticulum. *J Cell Biol* **168**, 389–399.

[29] Jiang CC, Yang F, Thorne RF, Zhu BK, Hersey P, and Zhang XZ (2009). Human melanoma cells under endoplasmic reticulum stress acquire resistance to microtubule-targeting drugs via XBP-1–mediated activation of Akt. *Neoplasia* **11**, 436–447.

[30] Kuwai T, Nakamura T, Sasaki T, Kim S-J, Fan D, Villares GJ, Zigler M, Wang H, Bar-Eli M, Kerbel RS, et al. (2008). Phosphorylated epidermal growth factor receptor on tumor-associated endothelial cells is a primary target for therapy with tyrosine kinase inhibitors. *Neoplasia* **10**, 489–500.

[31] Foss FM, Saleh MN, Krueger JG, Nichols JC, and Murphy JR (1998). Diphtheria toxin fusion proteins. *Clinical Applications of Immunotoxins.* AE Frankel (Ed.). Berlin, Germany: Springer-Verlag. pp. 63–81.

[32] Liu TF, Hall PD, Cohen KA, Willingham MC, Cai J, Thorburn A, and Frankel AE (2005). Interstitial diphtheria toxin-epidermal growth factor fusion protein therapy produces regressions of subcutaneous human glioblastoma multiforme tumors in athymic nude mice. *Clin Cancer Res* **11**, 329–334.

[33] Cohen KA (2003). Novel fusion protein therapy of refractory brain tumors. *Curr Pharm Biotechnol* **4**, 39–49.

[34] Theodoulou M and Baselga J (1995). Phase I dose escalation study of the safety, tolerability, pharmacokinetics and biologic effects of DAB_{389}-EGF in patient with solid malignances that express EGF receptors. *Proc ASCO* **14**, 480.

[35] Xue C, Wyckoff J, Liang F, Sidani M, Violini S, Tsai KL, Zhang ZY, Sahai E, Condeelis J, and Segall JE (2006). Epidermal growth factor receptor overexpression results in increased tumor cell motility *in vivo* coordinately with enhanced intravasation and metastasis. *Cancer Res* **66**, 192–197.

[36] Yang W, Barth RF, Wu G, Ciesielski MJ, Fenstermaker RA, Moffat BA, Ross BD, and Wikstrand CJ (2005). Development of a syngeneic rat brain tumor model expressing EGFRvIII and its use for molecular targeting studies with monoclonal antibody L8A4. *Clin Cancer Res* **11**, 341–350.

[37] Reilly RM, Kiarash R, Sandhu J, Lee YW, Cameron RG, Hendler A, Vallis K, and Gariépy J (2000). A comparison of EGF and MAb 528 labeled with ^{111}In for imaging human breast cancer. *J Nucl Med* **41**, 903–911.

[38] Hu M, Scollard D, Chan C, Chen P, Vallis K, and Reilly RM (2007). Effect of the EGFR density of breast cancer cells on nuclear importation, *in vitro* cytotoxicity, and tumor and normal-tissue uptake of [^{111}In]DTPA-hEGF. *Nucl Med Biol* **34**, 887–896.

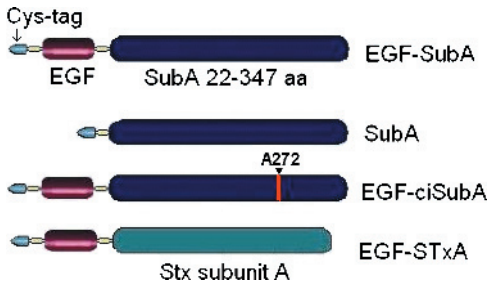

Figure W1. Construction of chimeric toxins. All proteins constructed for this study contain an N-terminal 15–amino acid cysteine-containing tag (Cys-tag) designed for site-specific conjugation of recombinant proteins [9,10]. For this work, we used a Cys-tag in EGF-SubA for site-specific modification with a maleimide derivative of Alexa Fluor 594. The resulting EGF-SubA* was used as a fluorescent tracer for cell microscopy and immunohistochemical experiments. Three control proteins were cloned in the same the pET/Hu-R4C$(G_4S)_3$ vector. **SubA:** To evaluate the toxicity of the nontargeted SubA protein, SubA was cloned in-frame with the Cys-tag as described in the Materials and Methods section for EGF-SubA, except without the EGF moiety. **EGF-ciSubA:** To confirm a causative role for SubA enzymatic activity in the toxic effects of EGF-SubA, we constructed an EGF-ciSubA protein containing catalytically inactive (ci) SubA. DNA encoding a catalytically inactive mutant of SubA with the S272A amino acid substitution was amplified by PCR from the pK184-subA$_{A272}$B plasmid described elsewhere [4]. **EGF-StxA:** To compare the effects of EGF-SubA with an EGF-based fusion toxin acting through different mechanism(s), we fused EGF to the full-length subunit A of Shiga toxin (StxA). DNA encoding StxA was amplified by PCR from the pJB144 plasmid (kindly provided by Dr. A. Soltyk, Samuel Lunfield Research Institute, Toronto, Canada) and cloned in-frame with EGF. Functional activity of EGF-StxA is shown in Figure W6. All four recombinant chimeric toxins were expressed in *E. coli* strain BL21(DE3), refolded from inclusion bodies and purified as described [9].

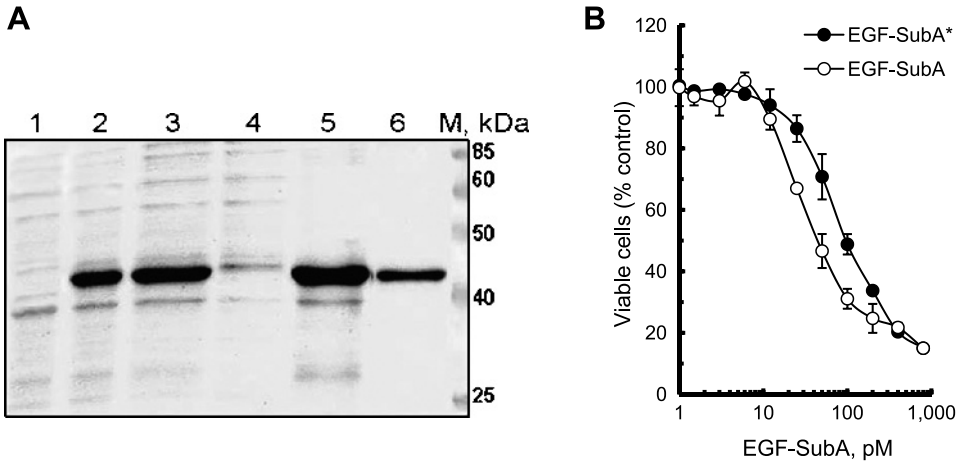

Figure W2. Expression, purification, and tissue culture testing of EGF-SubA. (A) SDS-PAGE analysis of bacterial expression and purification of EGF-SubA. Typical recovery and quality of purification by ion exchange chromatography (prepacked 1-ml Q-column; GE Healthcare) is shown. Samples were separated on 15% reducing gels and stained by SafeBlue stain (BioRad, Hercules, CA). Lanes: 1, uninduced culture; 2, isopropyl β-D-1-thiogalactopyranoside–induced culture; 3, total bacterial homogenate; 4, soluble part of bacterial homogenate; 5, insoluble part; 6, protein purified by ion exchange chromatography migrates as single prominent band with apparent molecular mass of 45 kDa. M, prestained molecular weight markers (BioRad). (B) Functional activity of EGF-SubA and fluorescent conjugate EGF-SubA* was tested on EGFR-positive breast cancer cells MDA231luc. Cells were plated in 96-well plates at 2000 cells per well 20 hours before the experiment. EGF-SubA and EGF-SubA* were diluted in complete culture medium and added to cells in triplicate wells. Cells were incubated under normal culture conditions for 72 hours and then viable cells were detected by CellTiter 96 AQueous One Solution Cell Proliferation assay (Promega).

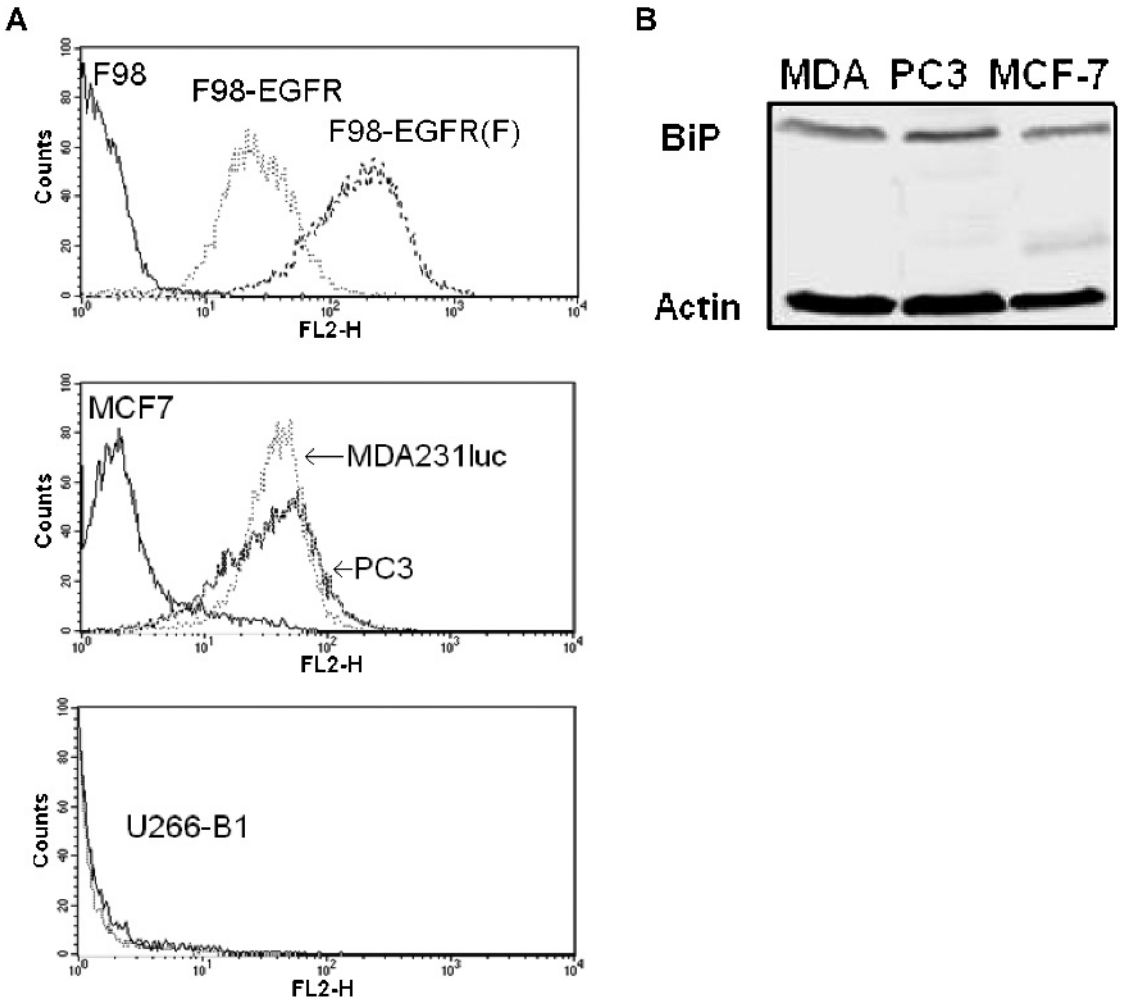

Figure W3. Expression of EGFR and BiP in cancer cells used in this study. (A) For estimation of EGFR expression, we used F98-EGFR and F98-EGFR(F) cells with known EGFR per cell (Table 1). Each cell line was incubated with a PE-labeled rat anti–human EGFR–specific antibody (AbCam), washed once with PBS buffer after a 30-minute incubation, and analyzed on a FACScan flow cytometer (Becton Dickinson, San Diego, CA) equipped with CELLQuest software. An irrelevant PE-labeled rat anti–human IL-10 (PharMingen, San Diego, CA) antibody was used as a negative control for the nonspecific binding of cells to PE-conjugated rat antibodies. (B) Cell lysates of untreated human cancer cells MDA231luc, PC3, and MCF-7 were made as described in the legend to Figure 1. Equal numbers of cell equivalents were analyzed side-by-side by Western blot analysis.

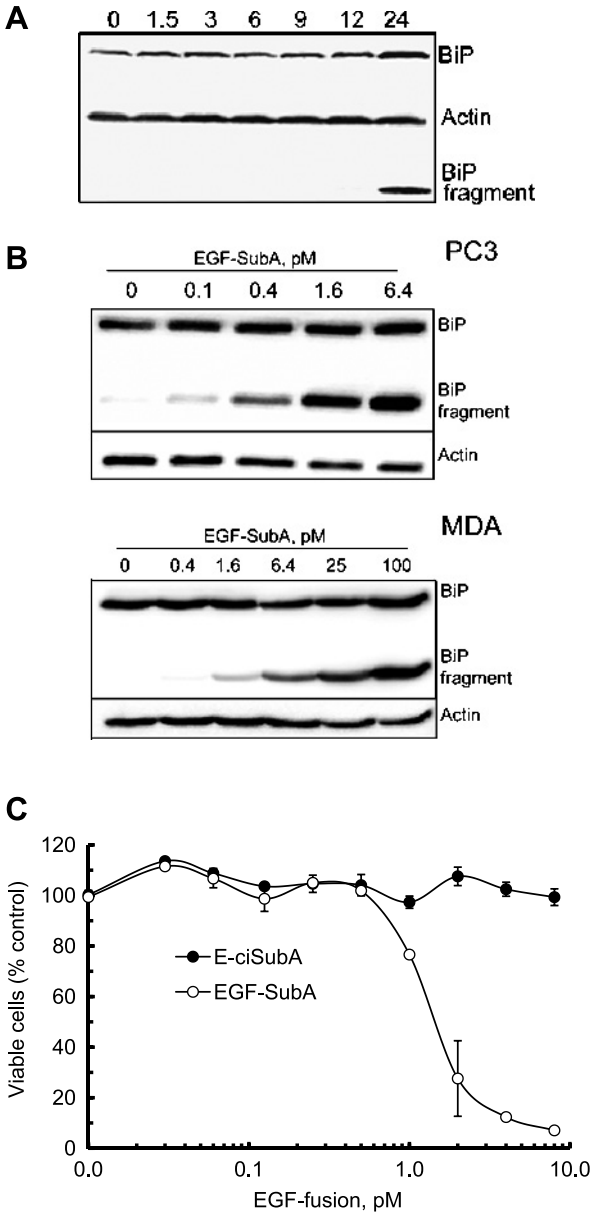

Figure W4. The pattern of EGF-SubA–induced BiP cleavage is cell-specific and critically depends on both EGF and SubA moieties. Cells were plated in six-well plates, 0.5 million/well and exposed to EGF-SubA 20 hours later. (A) MDA231luc cells were exposed to 1 nM SubA for the indicated times, lysed, and analyzed by Western blot analysis with BiP-specific antibody from Santa Cruz Biotechnology. (B) PC3 and MDA231luc cells were exposed to varying EGF-SubA concentrations for 72 hours, then lysed and analyzed by Western blot analysis with a BiP-specific antibody from R&D Systems. (C) EGF-ciSubA is not toxic for the most susceptible PC3 cells. PC3 were plated in 96-well plates at 2000 cells per well 20 hours before the experiment. EGF fusion proteins, EGF-SubA or EGF-ciSubA, were diluted in complete culture medium and added to cells in triplicate wells. Viable cells were determined 96 hours later by the CellTiter assay (Promega).

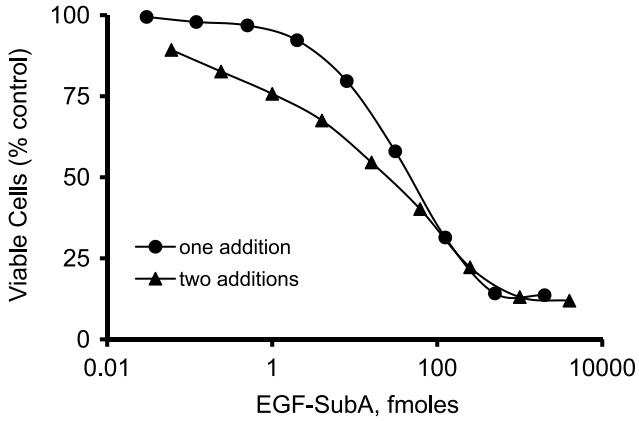

Figure W5. Fractional addition is more cytotoxic at low doses of EGF-SubA. MDA231luc cells were plated into 96-well plates at 2000 cells/50 μl per well. Twenty-four hours later, EGF-SubA was serially diluted in complete culture medium and added to cells in triplicate wells to a final volume of 0.1 ml/well. After a 24-hour incubation under normal culture conditions, EGF-SubA was added to cells scheduled to receive two doses of cytotoxin. EGF-SubA was serially diluted in complete culture medium and added to wells to double its concentration in each well and make a final volume of 0.15 ml/well. To maintain uniform volumes in all wells, cells exposed to single dose of EGF-SubA were supplemented with 50 μl per well of complete culture medium. After a total exposure of 114 hours, the numbers of viable cells were determined by the CellTiter assay (Promega).

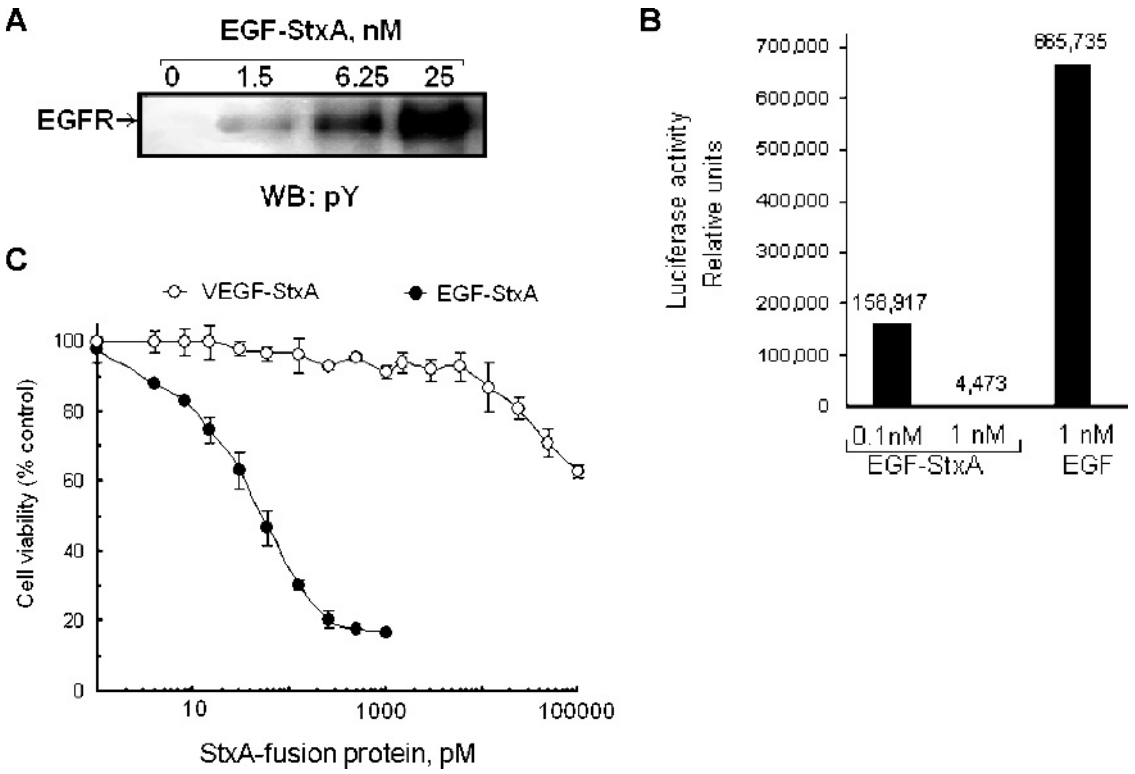

Figure W6. Functional activity of EGF-StxA. (A) Activity of EGF moiety was tested by the ability of EGF-StxA fusion protein to induce EGFR tyrosine autophosphorylation in F98-EGFR cells as described in legend to Figure 1*A*. (B) Because StxA inhibits protein synthesis by targeting 28S ribosomal RNA, functional activity of the StxA domain in EGF-StxA was tested by its ability to terminate *in vitro* translation of luciferase mRNA as described elsewhere [13]. The reaction was completely terminated in the presence of 1 nM EGF-StxA. The control reaction was incubated with bacterially expressed Cys-tagged EGF [10, and supplementary material herein]. (C) The ability to inhibit growth of MDA231luc cells was tested as described in the legend to Figure 2*B*. EGF-StxA inhibited MDA231luc cell growth with an IC_{50} of 60 $\pm$ 10 pM. The fusion protein containing StxA and an unrelated growth factor, human VEGF, was described elsewhere [13]. We used VEGF-StxA to compare EGFR-mediated and nonspecific StxA cytotoxicity for MDA231luc cells.

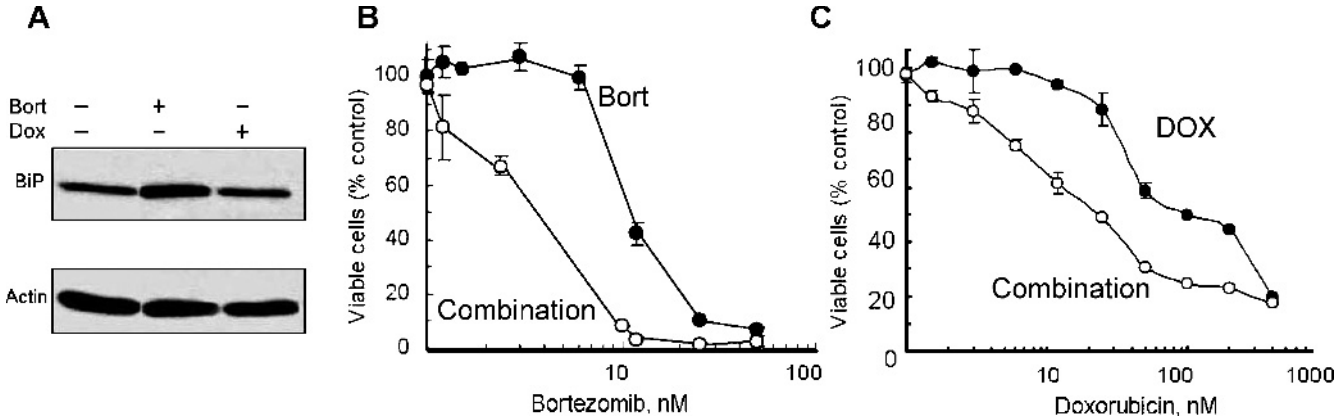

Figure W7. Lack of synergism in combinations of EGF-SubA with drugs that induce low to no up-regulation of GRP78/BiP. (A) BiP expression in MDA231luc cells after 24 hours of exposure to 2 μM bortezomib or 1 μM doxorubicin was analyzed as described in legend to Figure 2. (B) MDA231luc cells were exposed to bortezomib, alone (Bort) or in combination with EGF-SubA at a molar ratio of 2000:1. (C) MDA231luc cells were exposed to doxorubicin, alone (DOX) or in combination with EGF-SubA at a molar ratio of 1000:1. Cell viability was determined after 72 hours.